

# The crystal structures of pressure-induced LiSrAlF<sub>6</sub>-II and LiCaAlF<sub>6</sub>-II

Andrzej Grzechnik<sup>1,5</sup>, Vladimir Dmitriev<sup>2</sup>, Hans-Peter Weber<sup>2,3</sup>,  
Jean-Yves Gesland<sup>4</sup> and Sander van Smaalen<sup>1</sup>

<sup>1</sup> Laboratory of Crystallography, University of Bayreuth, D-95440 Bayreuth, Germany

<sup>2</sup> Group 'Structure of Materials under Extreme Conditions', Swiss–Norwegian Beamlines, European Synchrotron Radiation Facility, BP 220, F-38043 Grenoble cedex, France

<sup>3</sup> Laboratoire de Cristallographie, EPFL/SB/IPMC/LCR, École Polytechnique Fédérale de Lausanne, CH-1015 Lausanne, Switzerland

<sup>4</sup> Université du Maine-Cristallogénese, F-72025 Le Mans cedex, France

E-mail: andrzej@uni-bayreuth.de

Received 5 December 2003

Published 6 February 2004

Online at [stacks.iop.org/JPhysCM/16/1033](http://stacks.iop.org/JPhysCM/16/1033) (DOI: 10.1088/0953-8984/16/7/003)

## Abstract

The crystal structures of LiCaAlF<sub>6</sub>-II and LiSrAlF<sub>6</sub>-II (both  $P2_1/c$ ,  $Z = 4$ ) occurring at high pressures and room temperature were studied with synchrotron angle-dispersive x-ray powder diffraction in diamond anvil cells. The structure of LiSrAlF<sub>6</sub>-II stable between 1.6 and 3.0 GPa was solved with a global optimisation algorithm and group theory considerations, and refined with the Rietveld method in the rigid-body approximation. It is a distorted variant of the ambient pressure polymorph (LiSrAlF<sub>6</sub>-I,  $P\bar{3}1c$ ,  $Z = 2$ ), in which each cation occupies a deformed octahedral site. LiCaAlF<sub>6</sub> transforms to this monoclinic polymorph II above about 7 GPa. The differences in the high-pressure behaviours of LiCaAlF<sub>6</sub> and LiSrAlF<sub>6</sub> are discussed by considering the ionic radii.

## 1. Introduction

The *colquiriite* family of fluoride compounds LiMM'F<sub>6</sub> ( $M = \text{Ca or Sr}$ ;  $M' = \text{Al, Ga, or Cr}$ ) is considered to be the most promising class of materials for optical applications such as laser hosts and scintillating materials [1–9]. The crystal structure of LiSrAlF<sub>6</sub>-I ( $P\bar{3}1c$ ,  $Z = 2$ ) is an ordered derivative of the Li<sub>2</sub>ZrF<sub>6</sub> type ( $P\bar{3}1m$ ,  $Z = 1$ ) [10], with each cation occupying a deformed octahedral site within the hexagonal close packed arrangement of fluorine atoms. The polyhedral distortions in LiMM'F<sub>6</sub> have been correlated with the sizes of the  $M$  and  $M'$  cations [8, 10, 11]. For the  $M$  site occupied by luminescent dopants, the distortion, larger for the Sr compounds, is associated with the relative rotations of the two opposite

<sup>5</sup> Author to whom any correspondence should be addressed.

trigonal F faces. As a consequence, the strontium-containing materials provide larger optical absorption coefficients determined by the strengths of static and dynamic distortions of the crystal field [11].

Information on the high-pressure behaviour of the *colquiriite* compounds  $\text{LiMM}'\text{F}_6$  ( $M = \text{Ca}$  or  $\text{Sr}$ ;  $M' = \text{Al}$ ,  $\text{Ga}$ , or  $\text{Cr}$ ) is not available in the literature. At high pressures and high temperatures [12, 13],  $\text{Li}_2\text{ZrF}_6$  transforms into a polymorph with the  $\text{Li}_2\text{TbF}_6$  structure ( $P2_1/c$ ,  $Z = 4$ ) [14], in which the zirconium atoms have a bicapped trigonal prismatic coordination, forming edge-sharing chains along the  $a$  axis. The  $\text{Li}^{1+}$  cations are in two types of coordination: octahedra and square pyramids. This structure could be considered a distorted variant of the  $\gamma$ - $\text{Na}_2\text{UF}_6$  ordered *fluorite* ( $Immm$ ,  $Z = 2$ ), in which all the cations are surrounded by fluorines in a cube coordination [14]. In the course of our work on the high-pressure high-temperature behaviour of the *colquiriite* compounds  $\text{LiMM}'\text{F}_6$  ( $M = \text{Ca}$  or  $\text{Sr}$ ;  $M' = \text{Al}$  or  $\text{Ga}$ ), we found that  $\text{LiSrAlF}_6$  and  $\text{LiCaAlF}_6$  undergo a series of reversible pressure-induced structural transformations at room temperature. Here, we investigate the crystal structures of new polymorphs of  $\text{LiSrAlF}_6$  occurring below 3.0 GPa and of  $\text{LiCaAlF}_6$  formed above about 7 GPa. Additional pressure-induced polymorphs of  $\text{LiSrAlF}_6$  above 3 GPa will be the subject of a separate study.

## 2. Experimental details

Single crystals of  $\text{LiSrAlF}_6$  and  $\text{LiCaAlF}_6$ , grown by the Czochralski method, were ground into fine powders in ethanol and loaded into diamond anvil cells with argon or a silicon oil as the pressure transmitting medium. Angle-dispersive powder x-ray diffraction patterns were measured at room temperature on the Swiss–Norwegian Beamlines at the European Synchrotron Radiation Facility (BM1A, ESRF, Grenoble, France). Monochromatic radiation at  $0.71998 \text{ \AA}$  was used for data collection on image plate (MAR345). The images were integrated using the program FIT2D [15] to yield intensity versus  $2\theta$  diagrams. The ruby luminescence method [16] was used for pressure measurements. At ambient conditions, the measured patterns of  $\text{LiSrAlF}_6$  and  $\text{LiCaAlF}_6$  matched perfectly those calculated with the program PowderCell [17] using the structural data from Keszler and Schaffers [10]. The refined lattice parameters for  $\text{LiSrAlF}_6$  and  $\text{LiCaAlF}_6$  were  $a = 5.1022(1) \text{ \AA}$ ,  $c = 10.2563(1) \text{ \AA}$ ,  $V = 229.51(3) \text{ \AA}^3$ , and  $a = 4.9998(2) \text{ \AA}$ ,  $c = 9.6418(1) \text{ \AA}$ ,  $V = 208.73(3) \text{ \AA}^3$ , respectively.

## 3. Results and discussion

Diffraction patterns of  $\text{LiSrAlF}_6$  at selected pressures to 3.0 GPa are shown in figure 1. The diagrams measured between 1.6 and 3.0 GPa are due to a novel high-pressure polymorph of this compound, hereupon called  $\text{LiSrAlF}_6\text{-II}$ . The pattern collected at 1.6 GPa was used for structure determination. The first 20 reflections were indexed using the program DICVOL91 [18] with a monoclinic unit cell:  $a = 10.0560(7) \text{ \AA}$ ,  $b = 8.6197(6) \text{ \AA}$ ,  $c = 5.1367(4) \text{ \AA}$ ,  $\beta = 91.657(7)^\circ$ ,  $V = 445.1(2) \text{ \AA}^3$ ,  $M(20) = 32.1$ ,  $F(20) = 104.1(0.0035, 55)$ . The systematic absences indicated that the space group is  $P2_1/a$  (space group no 14) [19]. Unit cells with practically the same volumes,  $a \sin \beta$  factors, as well as  $b$  and  $c$  axial parameters were found by all the routines in the CRYSFIRE suite of indexing programs [20]. The other three diagrams collected at 1.9, 2.4, and 3.0 GPa (figure 1) were also indexed on this  $P2_1/a$  unit cell with related, i.e., pressure dependent (figure 2), lattice parameters using the programs DICVOL91 [18], ITO, and TREOR [20].

The crystal structure of  $\text{LiSrAlF}_6\text{-II}$  was partially solved from the pattern collected at 1.6 GPa in the standard  $P2_1/c$  ( $Z = 4$ ) setting of space group no 14 with the global optimisation

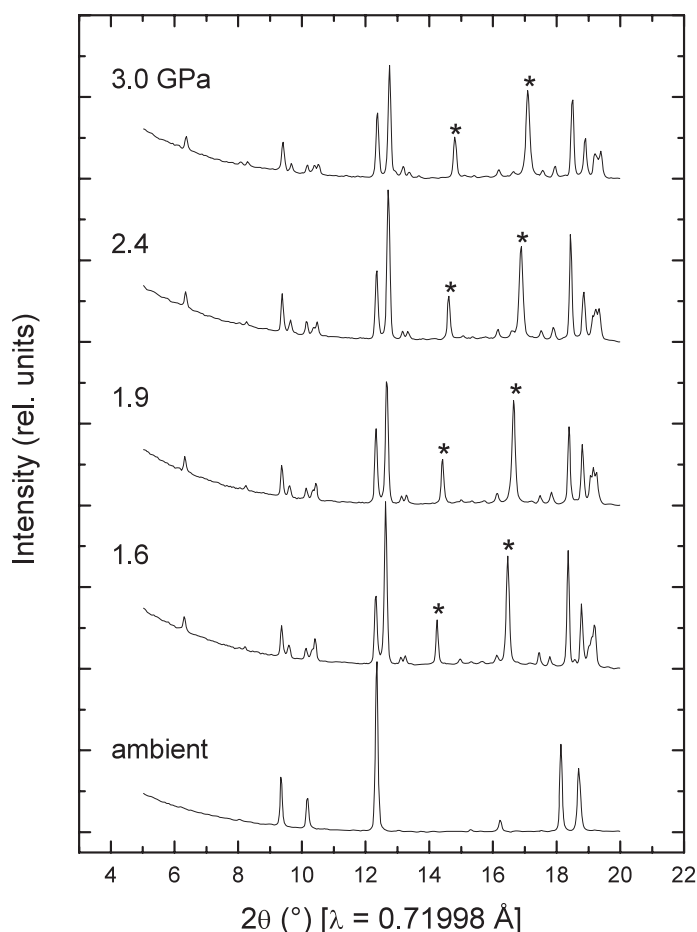


**Figure 1.** Selected powder patterns of LiSrAlF<sub>6</sub> upon compression with argon as a pressure medium. Reflections due to argon are marked with stars.

algorithm FOX [21]. The lattice parameters in the  $P2_1/c$  setting were refined with the Le Bail method [22] as  $a = 5.1346(6)$  Å,  $b = 8.6283(11)$  Å,  $c = 10.0598(12)$  Å, and  $\beta = 88.362(8)^\circ$ . Since the ratio of the number of observed Bragg peaks to the number of structural parameters was expected to be low (52 reflections, all atoms in the general positions 4e), the number of optimized parameters was drastically reduced by introducing an octahedron around the Al atoms with Al–F bond distances equal to 1.78–1.8 Å, i.e., equal to the distances in the ambient pressure structure ( $P\bar{3}1c$ ,  $Z = 2$ ) [10]. The solution was reached in about 50 000 trial configurations. However, the Li atoms could not be properly located using this method and some of the Li–F distances were anomalously short. The entire procedure was repeated without Li atoms and the resulting SrAlF<sub>6</sub><sup>-1</sup> sublattice was essentially identical. Also, the goodness-of-fit,  $R_{wp}$ , and  $R_p$  factors for the calculated and observed patterns were not different. The global optimisation of the LiSrAlF<sub>6</sub>-II structure against the diagram collected at 3.0 GPa with such a procedure yielded the same result. During all these procedures bonding and angular distortions of the AF<sub>6</sub> octahedra were accounted for by relaxing the delta and sigma parameters in the program FOX [21].

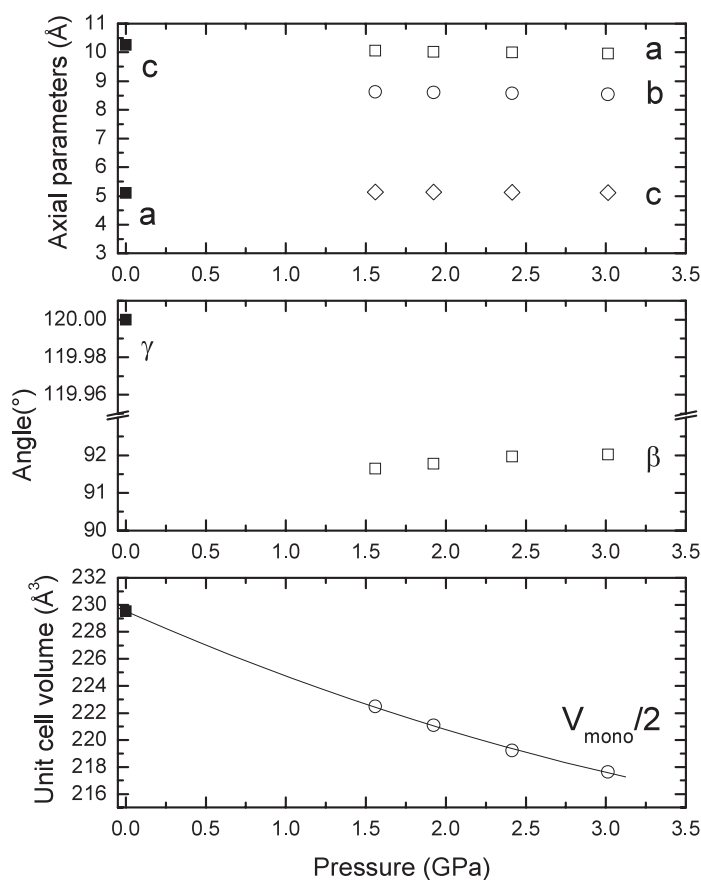


**Figure 2.** The pressure dependence of unit cell parameters and volumes in  $\text{LiSrAlF}_6$  to 3.0 GPa. Full and open symbols stand for the  $P\bar{3}1c$  ( $Z = 2$ ) and  $P2_1/a$  ( $Z = 4$ ) polymorphs, respectively. For clarity, the unit cell volumes of the monoclinic phase are divided by a factor of two. The line represents the equation-of-state fit to the unit cell volumes.

The detailed analysis of the globally optimised  $\text{SrAlF}_6^{-1}$  substructure in  $P2_1/c$  ( $Z = 4$ ) at 1.6 GPa indicated that it is similar to the one in the  $P\bar{3}1c$  ( $Z = 2$ ) structure at ambient conditions [10], with both  $\text{Sr}^{2+}$  and  $\text{Al}^{3+}$  cations in distorted octahedral coordination by fluorines. Exploring different possible routes for crystal structure transformations implemented in the program PowderCell [17], it appears that the transformation from the  $P\bar{3}1c$  ( $Z = 2$ ) to  $P2_1/c$  ( $Z = 4$ ) structures can be derived through the  $C2/c$  ( $Z = 4$ ) intermediate. The space group  $C2/c$  is the *translationengleiche* subgroup of  $P\bar{3}1c$  with the axis transformation  $(-a - b, a - b, c)$ . Furthermore, the space group  $P2_1/c$  is the *klassengleiche* subgroup (type IIa) of  $C2/c$  with the axis transformation  $(a, b, c)$ . The relationship between the hexagonal and monoclinic unit cell parameters is  $a_m \approx a_h$ ,  $b_m \approx \sqrt{3}a_h$ ,  $c_m \approx c_h$ , with  $\beta \approx 90^\circ$ . It turned out that the positional parameters for Sr, Al, and F atoms in  $P2_1/c$  ( $Z = 4$ ) transformed from the  $P\bar{3}1c$  ( $Z = 2$ ) structure approximated the ones from the structure solution with the global optimization method [21]. Therefore, the Li fractional coordinates in  $\text{LiSrAlF}_6\text{-II}$  ( $P2_1/c$ ,  $Z = 4$ ) were derived from the  $P\bar{3}1c$  ( $Z = 2$ ) structure by the same transformation.

The complete  $\text{LiSrAlF}_6\text{-II}$  structural model, i.e., the globally optimised  $\text{SrAlF}_6^{-1}$  substructure and the  $\text{Li}^{1+}$  cations from group theory considerations, was subsequently used for

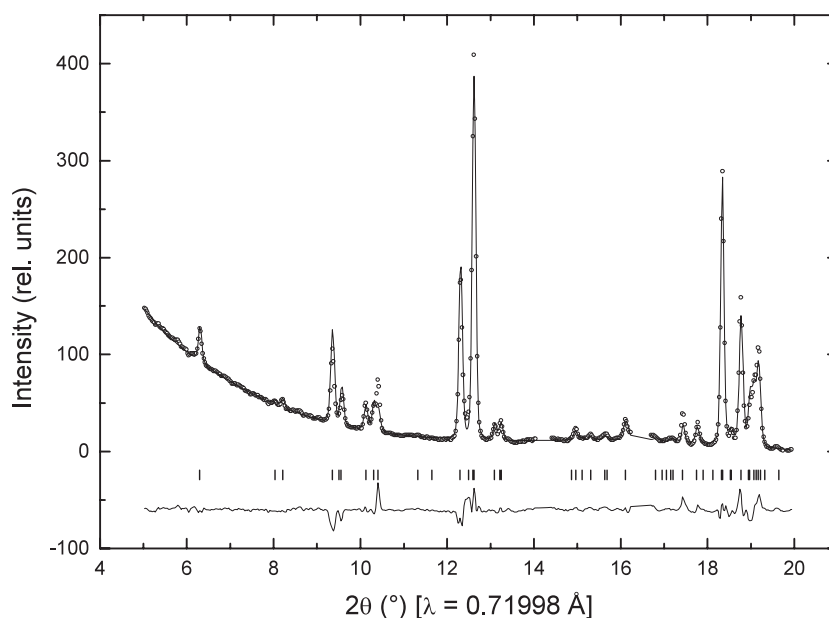


**Figure 3.** Observed, calculated, and difference x-ray powder patterns for LiSrAlF<sub>6</sub>-II ( $P2_1/c$ ,  $Z = 4$ ) at 1.6 GPa. Vertical markers indicate Bragg reflections. The  $2\theta$  regions  $14.05^\circ$ – $14.4^\circ$  and  $16.25^\circ$ – $16.7^\circ$ , in which two reflections due to argon are observed, were excluded from the Rietveld refinement.

the structure refinement against the observed pattern at 1.6 GPa with the Rietveld method, using the program GSAS [22] (figure 3). The best fit was obtained at  $R_{wp} = 12.15\%$ ,  $R_p = 9.0\%$ ,  $R_{prof} = 5.17\%$  (the residuals  $R_{wp}$  and  $R_p$  have been calculated with the background eliminated; see the GSAS manual). After a set of positional parameters for all the atoms had been inserted into the experimental file, the GEOMETRY subroutine was used to determine the orthonormal coordinates and rotation angles  $R_1(X)$ ,  $R_2(Y)$ , and  $R_3(Z)$  for the rigid octahedron centred at the Al<sup>3+</sup> cation. Introducing the AlF<sub>6</sub> polyhedron reduced the number of structural variables. The refined parameters for the rigid body were:  $R_1(X)$ ,  $R_2(Y)$ , and  $R_3(Z)$  rotation angles,  $T(X)$ ,  $T(Y)$ , and  $T(Z)$  translations, and an isotropic translational tensor ( $T_{11} = T_{22} = T_{33}$ ) in the TLS formalism. The additional variables were: Li and Sr atomic positions, lattice parameters, scale factor, and Stephens profile function [23]. The conventional fractional coordinates for all the atoms and selected interatomic distances are given in table 1.

The structure of LiSrAlF<sub>6</sub>-II in different crystallographic projections is shown in figure 4. It consists of deformed LiAlF<sub>6</sub> slabs, in which the Li and Al atoms occupy two thirds of octahedral sites in hexagonal close packing of fluorine atoms in the ( $a, b$ ) plane. The Sr atoms are sandwiched between the slabs on the octahedral sites. The LiF<sub>6</sub> and AlF<sub>6</sub> polyhedra share edges with each other and vertices with the SrF<sub>6</sub> polyhedra. This structure is a distorted variant of parent LiSrAlF<sub>6</sub>-I ( $P\bar{3}1c$ ,  $Z = 2$ ) with the same stacking sequence  $\cdots F(\text{Li, Al})\text{FSrF} \cdots$  along the  $c$  axis [10]. The pressure-induced structure of LiSrAlF<sub>6</sub>-II ( $P2_1/c$ ,  $Z = 4$ ) arises from distortions of hexagonal close packing of the fluorine atoms (figures 4 and 5). The comparison of the octahedra around the Sr atoms in the low- and high-pressure phases is shown in figure 5. In the *colquiriite* structure ( $P\bar{3}1c$ ,  $Z = 2$ ), the twisting of the trigonal F planes perpendicular to the  $C_3$  symmetry axis can be described by an angular deviation  $\Delta\theta$  from the ideal value of  $60^\circ$ , that is  $7.2^\circ$  in LiSrAlF<sub>6</sub>-I [10]. The octahedral distortion in LiSrAlF<sub>6</sub>-II ( $P2_1/c$ ,  $Z = 4$ ) can no longer be described by only one  $\Delta\theta$  parameter since pairs

**Table 1.** Structural parameters of LiSrAlF<sub>6</sub>-II ( $P2_1/c$ ,  $Z = 4$ ) at 1.6 GPa— $a = 5.1346(6)$  Å,  $b = 8.6283(11)$  Å,  $c = 10.0598(12)$  Å,  $\beta = 88.362(8)^\circ$ . Estimated standard deviations are given in parentheses.

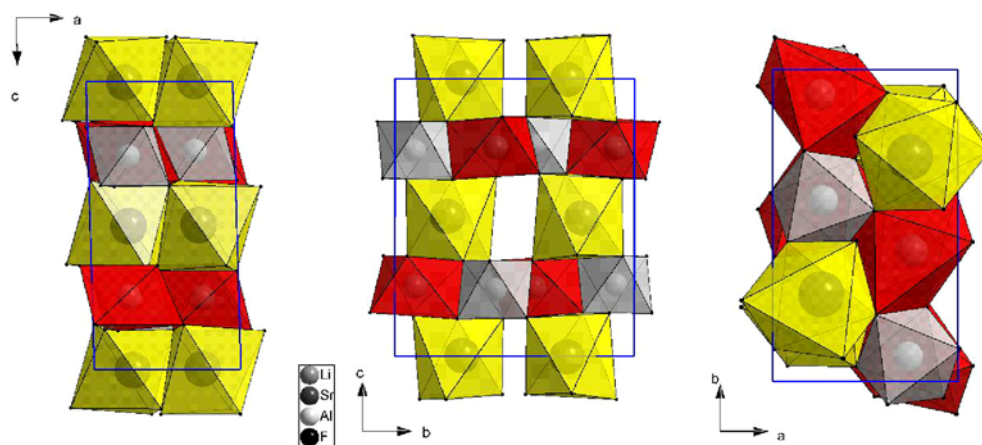
Atom	$x$	$y$	$z$
Li	0.25(6)	0.581(24)	0.249(27)
Sr	0.2613(24)	0.2195(9)	0.5024(18)
Al	0.271(5)	0.5804(28)	0.7594(19)
F1	0.169(6)	0.7392(34)	0.8654(31)
F2	0.549(6)	0.5476(40)	0.8621(25)
F3	0.444(6)	0.7141(35)	0.6565(28)
F4	−0.010(6)	0.6045(41)	0.6563(25)
F5	0.079(6)	0.4483(34)	0.8614(27)
F6	0.382(7)	0.4259(35)	0.6559(29)

Selected distances (Å)			
Li–F1	1.97(22)	Li–F2	1.87(25)
Li–F3	2.22(22)	Li–F4	2.22(24)
Li–F5	2.06(29)	Li–F6	2.15(29)
(Li–F)	2.08		
Sr–F1	2.555(28)	Sr–F2	2.254(33)
Sr–F3	2.242(26)	Sr–F4	2.578(31)
Sr–F5	2.250(31)	Sr–F6	2.448(29)
(Sr–F)	2.43		
Al–F1	1.803 62(16)	Al–F2	1.811 79(19)
Al–F3	1.774 37(15)	Al–F4	1.809 81(19)
Al–F5	1.807 44(15)	Al–F6	1.776 00(16)
(Al–F)	1.80		
F1–F2	2.557 47(22)	F1–F3	2.507 61(28)
F1–F4	2.594 52(24)	F1–F5	2.554 05(32)
F2–F3	2.587 24(23)	F2–F5	2.566 03(27)
F2–F6	2.500 19(24)	F3–F4	2.517 42(26)
F3–F6	2.507 95(32)	F4–F5	2.516 24(23)
F4–F6	2.532 55(22)	F5–F6	2.559 86(28)
(F–F)	2.54		

of opposite F planes in the SrF<sub>6</sub> octahedra are not parallel to each other any more. This new structure of LiSrAlF<sub>6</sub> ( $P2_1/c$ ,  $Z = 4$ ) is different from the monoclinic structures ( $P2_1/c$ ,  $Z = 4$ ) of LiBaMF<sub>6</sub> ( $M = \text{Al, Ga, Cr, V, Fe, Ti}$ ) containing icosahedra of BaF<sub>12</sub> within a framework of isolated LiF<sub>4</sub> tetrahedra and MF<sub>6</sub> octahedra mutually linked by corners [24]. It also does not bear any resemblance to the high-pressure high-temperature structure ( $P2_1/c$ ,  $Z = 4$ ) of parent Li<sub>2</sub>ZrF<sub>6</sub> [13], with the zirconium atoms in edge-sharing bicapped trigonal prisms along the  $a$  axis and the lithium atoms in two types of coordination: octahedra and square pyramids.

The pressure dependence of the lattice parameters in the hexagonal and monoclinic polymorphs of LiSrAlF<sub>6</sub> is plotted up to about 3 GPa in figure 2. The compression data for both  $P\bar{3}1c$  ( $Z = 2$ ) and  $P2_1/a$  ( $Z = 4$ ) polymorphs to 3 GPa could be fitted together by the Birch equation of state  $P(V) = 1.5B_0(x^{-7} - x^{-5})(1 - y)$ , where  $x = (V/V_0)^{1/3}$  and  $y = 0.75(4 - B')(x^{-2} - 1)$  [25]. Since the number of data points for such a small pressure range was limited, the first derivative of the bulk modulus  $B'$  and the  $V_0$  unit cell volume of LiSrAlF<sub>6</sub> at ambient pressure were fixed to 4.0 and 229.51 Å<sup>3</sup>, respectively, and not refined.



**Figure 4.** The crystal structure of LiSrAlF<sub>6</sub>-II ( $P2_1/c$ ,  $Z = 4$ ).  
(This figure is in colour only in the electronic version)

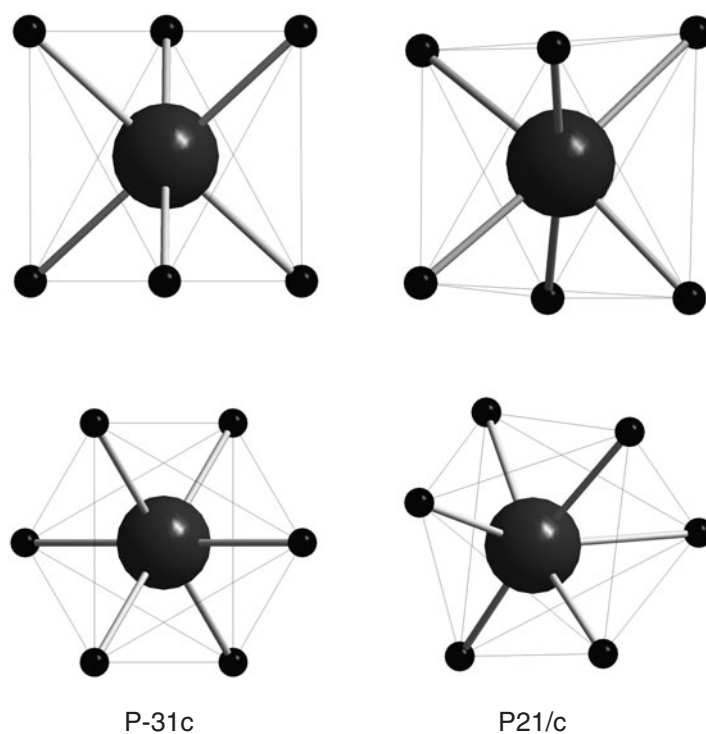


**Figure 5.** Coordination polyhedra around the Sr atoms in the  $P\bar{3}1c$  (left) and  $P2_1/c$  (right) polymorphs of LiSrAlF<sub>6</sub>.

The resulting zero-pressure bulk modulus  $B_0$  is 49(1) GPa, assuming that the  $P2_1/a$  ( $Z = 4$ ) unit cell volumes are divided by a factor of two.

Diffraction patterns of LiCaAlF<sub>6</sub> at selected pressures with a silicon oil or argon as the pressure transmitting medium are shown in figures 6 and 7, respectively. Regardless

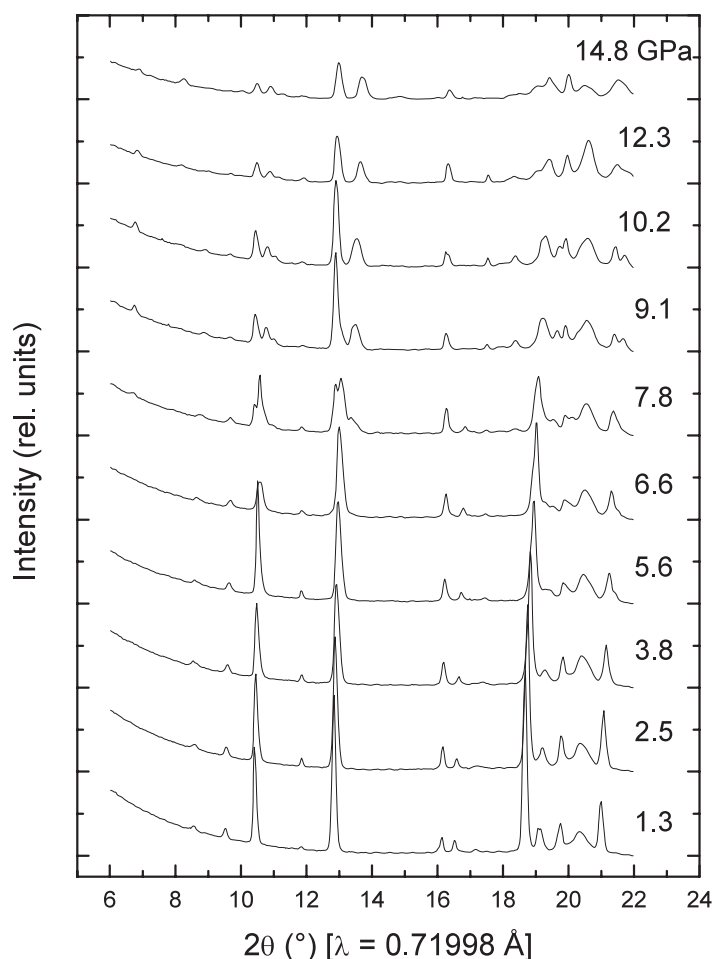


**Figure 6.** Selected powder patterns of  $\text{LiCaAlF}_6$  upon compression with a silicon oil as a pressure medium.

of the medium, a fully reversible pressure-induced phase transition in this material takes place above 7 GPa. The low- and high-pressure phases coexist in the range from 7 to about 9 GPa. The first 20 reflections of the pattern collected at 9.1 GPa with argon were indexed using the program DICVOL91 [18] with a monoclinic unit cell:  $a = 5.0136(5) \text{ \AA}$ ,  $b = 8.1588(7) \text{ \AA}$ ,  $c = 9.1821(9) \text{ \AA}$ ,  $\beta = 93.08(1)^\circ$ ,  $V = 375.0(2) \text{ \AA}^3$ ,  $M(20) = 21.6$ ,  $F(20) = 50.2(0.0056, 68)$ . The systematic absences indicated that the space group is  $P2_1/c$  (space group no 14) [19]. The same unit cell was found by the program TREOR in the CRYSFIRE suite of indexing programs [20]. The unit cell parameters and space group  $P2_1/c$  ( $Z = 4$ ) suggest that the new structure of  $\text{LiCaAlF}_6$  is of the  $\text{LiSrAlF}_6$ -II type. Indeed, the calculated pattern with the  $\text{LiSrAlF}_6$ -II structural model matches very well the measured one at 9.1 GPa with argon. In addition, a global optimization method [21] on this diagram yielded the  $\text{CaAlF}_6^{-1}$  sublattice like the  $\text{SrAlF}_6^{-1}$  one in  $\text{LiSrAlF}_6$ -II. However, broadening of the observed x-ray reflections precluded any reliable Rietveld refinement [22]. This new polymorph of  $\text{LiCaAlF}_6$  is stable at least up to about 16 GPa (figure 7).

The pressure dependence of the lattice parameters in the hexagonal and monoclinic polymorphs of  $\text{LiCaAlF}_6$  is plotted in figure 8, assuming that the  $P2_1/c$  ( $Z = 4$ ) unit cell

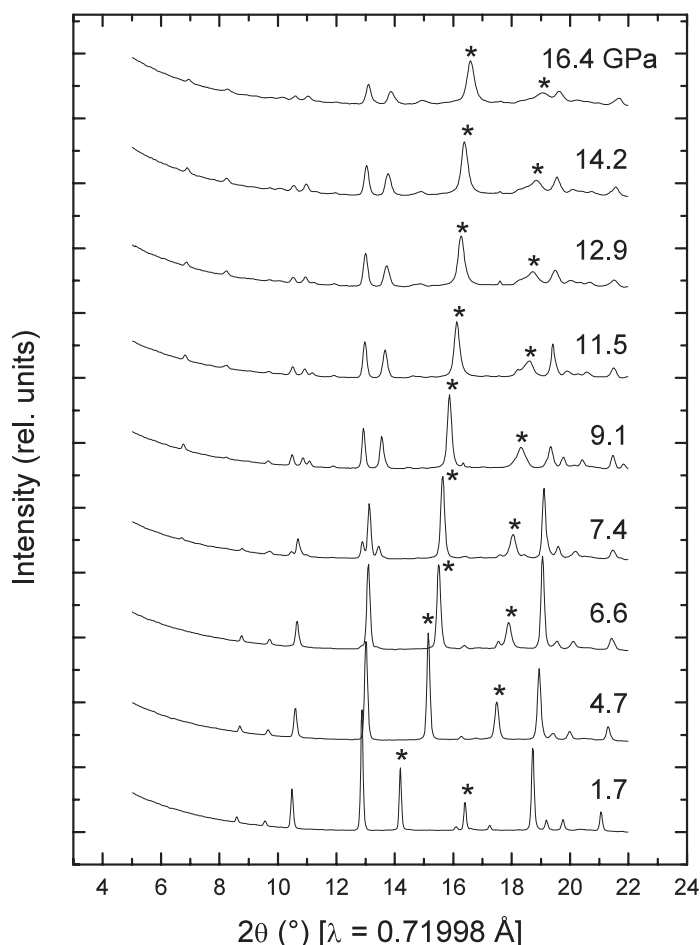


**Figure 7.** Selected powder patterns of LiCaAlF<sub>6</sub> upon compression with argon as a pressure medium. Reflections due to argon are marked with stars.

volumes are divided by a factor of two. The compression data for the  $P\bar{3}1c$  ( $Z = 2$ ) polymorph were fitted by the Birch equation of state [25] with the first derivative of the bulk modulus  $B'$  and the  $V_0$  unit cell volume of LiCaAlF<sub>6</sub> at ambient pressure fixed to 4.0 and 208.73 Å<sup>3</sup>, respectively, and not refined. The resulting zero-pressure bulk modulus  $B_0$  is 93(4) GPa. All the compression data for both the hexagonal and monoclinic polymorphs cannot be fitted by a common equation of state since there is a discontinuity in the evolution of the unit cell volumes at the phase transition  $P\bar{3}1c$  ( $Z = 2$ )  $\rightarrow$   $P2_1/c$  ( $Z = 4$ ).

#### 4. Concluding remarks

The combination of a global optimisation [21] and group theory [17] with the Rietveld method [22] allowed for the solution and refinement of the crystal structure of high-pressure LiSrAlF<sub>6</sub>-II ( $P2_1/c$ ,  $Z = 4$ ) from x-ray powder diffraction data. Important for the successful solution and refinement was the introduction of the rigid-body geometrical constraints to AlF<sub>6</sub> octahedral units, resulting in a reduced number of structural variables. The structure of the

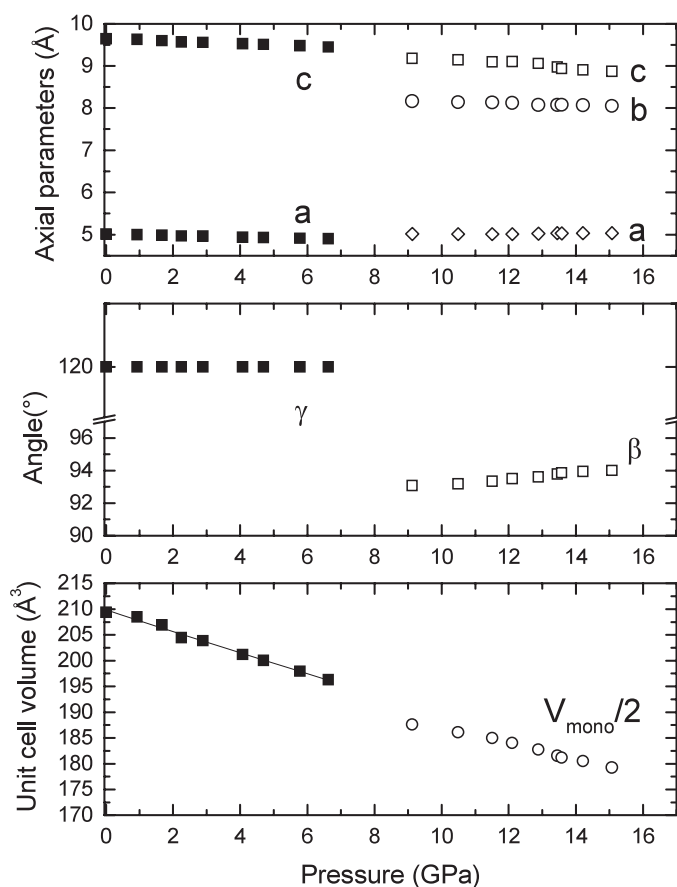


**Figure 8.** The pressure dependence of unit cell parameters and volumes in  $\text{LiCaAlF}_6$ . Full and open symbols stand for the  $P\bar{3}1c$  ( $Z = 2$ ) and  $P2_1/a$  ( $Z = 4$ ) polymorphs, respectively. For clarity, the unit cell volumes of the monoclinic phase are divided by a factor of two. The line represents the equation-of-state fit to the unit cell volumes. The data for the two phases coexisting in the pressure range 7–9 GPa are not plotted.

$\text{LiSrAlF}_6$ -II polymorph ( $P2_1/c$ ,  $Z = 4$ ) below 3.0 GPa is a distorted variant of  $\text{LiSrAlF}_6$ -I ( $P\bar{3}1c$ ,  $Z = 2$ ) and consists of deformed  $\text{LiAlF}_6$  slabs, in which the Li and Al atoms occupy two thirds of the octahedral sites in hexagonal close packing of fluorine atoms. This  $\text{LiSrAlF}_6$ -II-type structure type is also taken by  $\text{LiCaAlF}_6$  at pressures exceeding 7 GPa and is stable at least up to about 16 GPa.

The stability and distortions of the *colquiriite* structure at atmospheric conditions have been previously discussed on a basis of ionic radii [8, 10, 11]. The  $\text{Ca}^{2+}$  and  $\text{Sr}^{2+}$  cations are octahedrally coordinated to fluorines. The octahedral distortions are larger for the Sr compounds and are associated with the relative rotations of the two opposite trigonal F faces. The compounds  $\text{LiBaMF}_6$  ( $M = \text{Al, Ga, Cr, V, Fe, Ti}$ ) do not possess the *colquiriite* structure ( $P2_1/c$ ,  $Z = 4$ ) as icosahedra of  $\text{BaF}_{12}$  are within a framework of isolated  $\text{LiF}_4$  tetrahedra and  $\text{MF}_6$  octahedra linked by corners [24]. Another structural type is encountered in  $\text{LiSmAlF}_6$  ( $P6_322$ ,  $Z = 2$ ) that is derived from the  $\text{LiSrAlF}_6$ -I type ( $P\bar{3}1c$ ,  $Z = 2$ ), however with  $\text{Sm}^{2+}$  in a trigonal prismatic coordination to fluorine atoms [26]. Accordingly, the observation that up to 3.0 GPa  $\text{LiSrAlF}_6$  has the  $P2_1/c$  ( $Z = 4$ ) structure with all the cations in the octahedral

coordination while LiCaAlF<sub>6</sub> transforms to the same type above 7 GPa could be explained with the 'ionic radii' argument. Similar distortions in the hexagonal close packing of fluorines and coordination units of the cations like the ones in LiSrAlF<sub>6</sub>-II (*P*2<sub>1</sub>/*c*, *Z* = 4) may be expected at low temperatures and atmospheric pressure to explain the anomalies in electron spin-resonance spectra of the solid solution LiSr<sub>*x*</sub>Ca<sub>1-*x*</sub>AlF<sub>6</sub> [11].

### Acknowledgment

Experimental assistance from the staff of the Swiss–Norwegian Beamlines at ESRF is gratefully acknowledged.

### References

- [1] Burkhalter R, Dohnke I and Hulliger J 2001 *Prog. Cryst. Growth Charact.* **42** 1
- [2] Joubert M F *et al* 2001 *J. Fluor. Chem.* **107** 235
- [3] Wells J P R *et al* 2000 *J. Lumin.* **87–89** 1029  
Tigreat P Y *et al* 2001 *J. Lumin.* **94/95** 23
- [4] Shimamura K *et al* 2002 *Opt. Mater.* **19** 109
- [5] Braud A *et al* 2000 *Phys. Rev. B* **61** 5280  
Braud A *et al* 2001 *Appl. Phys. B* **72** 909
- [6] Machado M A C *et al* 2002 *J. Phys.: Condens. Matter* **14** 271
- [7] Liu Z *et al* 2002 *Opt. Mater.* **19** 123
- [8] Ono Y *et al* 2001 *J. Cryst. Growth* **229** 505  
Pawlak D A *et al* 2001 *J. Cryst. Growth* **233** 699
- [9] Klimm D and Reiche P 1999 *Cryst. Res. Technol.* **34** 145  
Sato H *et al* 2002 *Japan. J. Appl. Phys.* **41** 2028
- [10] Schaffers K I and Keszler D A 1991 *Acta Crystallogr. C* **47** 18  
Yin Y and Keszler D A 1992 *Chem. Mater.* **4** 645
- [11] Yamada M *et al* 1999 *J. Phys.: Condens. Matter* **11** 10499  
Martínez Vázquez R *et al* 2002 *J. Cryst. Growth* **237–239** 894
- [12] Demazeau G, Menil F, Portier J and Hagenmuller P 1971 *C. R. Acad. Sci. C* **273** 1641
- [13] Grzechnik A and Gesland J-Y 2003 *Z. Kristallogr. NCS* **218** 3
- [14] Lalligant Y, Le Bail A, Ferey G, Avignand D and Cousseins J C 1988 *Eur. J. Solid State Inorg. Chem.* **25** 551  
Guillot M, El-Ghozzi M, Avignand D and Ferey G 1992 *J. Solid State Chem.* **97** 400
- [15] Hammersley A P, Svensson S O, Hanfland M, Fitch A N and Häusermann D 1996 *High Pressure Res.* **14** 235
- [16] Piermarini G J, Block S, Barnett J D and Forman R A 1975 *J. Appl. Phys.* **46** 2774  
Mao H K, Xu J and Bell P M 1986 *J. Geophys. Res.* **91** 4673
- [17] Kraus W and Nolze G 1998 *CPD Newsletter No. 20* International Union of Crystallography
- [18] Boulton A and Louer D 1991 *J. Appl. Crystallogr.* **24** 987
- [19] Laugier J and Bochu B *CHEKCELL* <http://www.inpg.fr/LMGP>
- [20] Shirley R 2002 *The Crysfire 2002 System for Automatic Powder Indexing: User's Manual* (Guildford: The Lattice Press)
- [21] Favre-Nicolin V and Cerny R 2002 *J. Appl. Crystallogr.* **35** 734
- [22] Larson A C and von Dreele R B 2000 *GSAS: General Structure Analysis System* Los Alamos National Laboratory
- [23] Stephens P W 1999 *J. Appl. Crystallogr.* **32** 281
- [24] Babel D 1974 *Z. Anorg. Allg. Chem.* **406** 23  
Viebahn W and Babel D 1974 *Z. Anorg. Allg. Chem.* **406** 38
- [25] Birch F 1978 *J. Geophys. Res.* **83** 1257
- [26] Köhler J and Müller B G 1991 *Z. Anorg. Allg. Chem.* **606** 169